

Version 3.2

## Search for a light Higgs boson in $\gamma\gamma$ final states at DØ

The DØ Collaboration  
URL <http://www-d0.fnal.gov>  
(Dated: March 8, 2008)

This note describes a search for a light Higgs boson in the di-photon final state in  $2.27 \pm 0.14$   $fb^{-1}$  of the DØ Run II data, collected from July 2002 to August 2007. Good agreement between the data and the standard model background prediction is observed. Since there is no evidence for new physics, we set 95% C.L. limits on the production cross section times the branching ratio ( $h \rightarrow \gamma\gamma$ ) for standard model like Higgs for different assumed Higgs masses.

*Preliminary Results for Winter 2008 Conferences*

## I. INTRODUCTION

In the standard model (SM), the  $h \rightarrow \gamma\gamma$  branching ratio is small, for instance, the value for a Higgs boson with a mass of 130 GeV is 0.22%. However, it is well-known that the SM is incomplete. In some models beyond the SM, the  $h \rightarrow \gamma\gamma$  branching ratio can be enhanced significantly, some examples can be found in [1]. The idea of the fermiophobic Higgs, which assumes zero couplings of the Higgs to the fermions, has been tested at LEP [2] - [5] and the Tevatron [6]. In this note, we take a more model-independent approach and search for a Higgs boson with fewer assumptions about the production mechanisms and decay branching ratios. We examine the inclusive di-photon dataset ( $\gamma\gamma+X$ ) and search for high mass resonances. The standard model Higgs is used as a possible signal model. The result of the search is interpreted as upper limits on the production cross section times the branching ratio ( $h \rightarrow \gamma\gamma$ ) for different assumed Higgs masses.

There are three major sources of background: (i) Drell-Yan events, when both electrons are misidentified as photons due to tracking inefficiencies, is estimated using Monte Carlo simulations; (ii) direct QCD di-photon events, estimated by Monte Carlo; (iii)  $\gamma + jet$  and  $jet + jet$  events, where the jet(s) are mis-identified as photon(s), is estimated from data.

## II. DØ DETECTOR AND DATA SAMPLE

The DØ detector is comprised of a central tracking system in a 2 T superconducting solenoidal magnet, a liquid-argon/uranium calorimeter, and a muon spectrometer [7]. The major parts of the DØ detector used in event selection are tracking system and electromagnetic (EM) calorimeter. The tracking system consists of a silicon microstrip tracker (SMT) and an eight-layer scintillating fiber tracker (CFT) mounted on thin coaxial barrels. It provides coverage for charged particles in the pseudorapidity range  $|\eta| < 3$  (where the pseudorapidity is defined as  $\eta \equiv -\ln[\tan(\frac{\theta}{2})]$ , with  $\theta$  denoting the polar angle with respect to the proton beam direction.) The calorimeter has a central section (CC) covering up to  $|\eta| \approx 1.1$ , and two end components (EC) extending coverage to  $|\eta| \approx 4.2$ . Each is housed in a separate cryostat. Each section is divided into EM layers on the inside and hadronic layers on the outside. The EM calorimeter has four longitudinal layers and transverse segmentation of  $0.1 \times 0.1$  in  $\eta - \phi$  space (where  $\phi$  is the azimuthal angle), except in the third layer, where it is  $0.05 \times 0.05$ . Luminosity is measured using plastic scintillator arrays located in front of the EC cryostats, covering  $2.7 < |\eta| < 4.4$ . The data acquisition system consists of a three-level trigger, designed to accommodate the high instantaneous luminosity. For final states containing two photon candidates with transverse momentum ( $p_T$ ) above 25 GeV, the trigger efficiency is close to 100%. The data samples used in this analysis were collected between July 2002 and August 2007 and corresponds to an integrated luminosity of  $2.27 \pm 0.14 fb^{-1}$ .

## III. EVENT SELECTION

In this analysis, at least two photon candidates in the central calorimeter region are selected in each event, and the leading and sub-leading  $p_T$  photon candidates must satisfy: (i)  $p_T > 25.0$  GeV; (ii) at least 97% of the cluster energy be deposited in the EM section of the calorimeter; (iii) the calorimeter isolation variable ( $I$ ) must be less than 0.1, where  $I \equiv \frac{E_{tot}(0.4) - E_{EM}(0.2)}{E_{EM}(0.2)}$ ,  $E_{tot}(0.4)$  is the total shower energy in a cone of radius 0.4, and  $E_{EM}(0.2)$  the EM energy in a cone of radius 0.2 around the electron candidate direction; (iv) no track pointing to the photon candidates; (v) the artificial neural network (ANN) output variable  $O_{NN}$  must be greater than 0.2, where the  $O_{NN}$  is an ANN discriminant variable that combines 3 characteristic variables of the EM showers: 1) the fraction of EM cluster energy deposited at the first layer of the EM calorimeter, 2) the number of cells in the first EM layer in cone 0.2, and 3) the scalar sum of transverse momenta of the tracks in an annular cone  $0.05 < \Delta R < 0.4$ . The  $O_{NN}$  is trained with  $Z \rightarrow ee$  data samples and multi-jet data samples using the JETNET package [8]. It was tested on the  $Z \rightarrow ee$  MC samples and jet MC samples. We directly use the electron  $O_{NN}$  on the photons. The  $O_{NN}$  distributions for the electron candidates from  $Z \rightarrow ee$  events in both data and MC samples, the photon candidates in the QCD di-photon MC samples and the fake photon candidates in jet MC samples are compared in Fig. 1. A cut  $O_{NN} > 0.2$  is made to suppress a significant amount of the background while maintaining almost 100% efficiency for the signal events. The efficiency of the ID cuts (denoted as i,ii, iii above) is determined from the  $Z \rightarrow ee$  data sample to be 90% - 92%. The efficiency of "no-track" requirement is 90% - 93%.

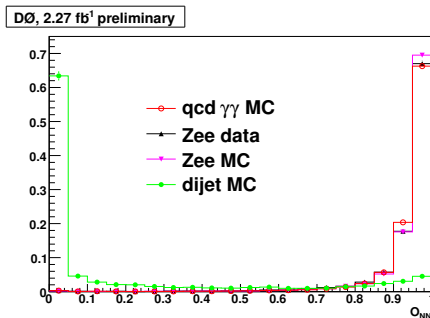


FIG. 1: Normalized distributions of photon  $O_{NN}$  output value from signal and background.

#### IV. BACKGROUNDS

There are three major sources of background, (i) Drell-Yan events, where both electrons are misidentified as photons; (ii) direct QCD di-photon events; (iii)  $\gamma + jet$  and  $jet + jet$  events where the jet(s) are mis-identified as photon(s).

We use  $Z/\gamma^* \rightarrow ee$  PYTHIA [9] Monte Carlo samples to estimate its contribution. The next-to-next-to-leading-order (NNLO)  $p\bar{p} \rightarrow Z \rightarrow ee$  cross section of  $254 \pm 10$  pb [10] for 60 - 130 GeV Z mass region is used for the absolute normalization. From the  $Z \rightarrow ee$  MC samples, we evaluate that 3.9% - 6.5% of the electrons can satisfy the photon selection requirements described in Section III due to the tracking inefficiencies. The total background contribution from Drell Yan process is found to be  $755.6 \pm 87.1$ .

We estimate the direct QCD di-photon contribution from PYTHIA MC using the NLO cross section from DIPHOX [11] for the absolute normalization, where 20% cross section uncertainty from the differences resulting from the different PDF and scale choices is adopted. The total contribution from QCD di-photon production in  $\gamma\gamma$  mass interval (50 GeV, 250 GeV) is  $3400.5 \pm 711.0$ .

We estimate the contributions from  $\gamma + jet$  and  $jet + jet$  events from real data by using a  $4 \times 4$  matrix background subtraction method. The method is described in detail in section 6.5 of [12]. In this analysis, we use an  $O_{NN} > 0.85$  cut to classify the candidates in 4 categories:

- $N_{pp}$  of them have both photon candidates pass the  $O_{NN}$  cut ;
- $N_{pf}$  of them have the first photon candidate pass the  $O_{NN}$  cut, but the second fail;
- $N_{fp}$  vice versa;
- $N_{ff}$  of them both photon candidates fail the  $O_{NN}$  cut.

This pass-fail 4-vector is related to the  $(N_{\gamma\gamma}, N_{\gamma j}, N_{j\gamma}, N_{jj})$  vector as follows:

$$\begin{pmatrix} N_{ff} \\ N_{fp} \\ N_{pf} \\ N_{pp} \end{pmatrix} = E \times \begin{pmatrix} N_{jj} \\ N_{jg} \\ N_{gj} \\ N_{gg} \end{pmatrix} \quad (1)$$

The  $4 \times 4$  matrix E is defined as:

$$\begin{pmatrix} (1 - \epsilon_{j1})(1 - \epsilon_{j2}) & (1 - \epsilon_{j1})(1 - \epsilon_{g2}) & (1 - \epsilon_{g1})(1 - \epsilon_{j2}) & (1 - \epsilon_{g1})(1 - \epsilon_{g2}) \\ (1 - \epsilon_{j1})\epsilon_{j2} & (1 - \epsilon_{j1})\epsilon_{g2} & (1 - \epsilon_{g1})\epsilon_{j2} & (1 - \epsilon_{g1})\epsilon_{g2} \\ \epsilon_{j1}(1 - \epsilon_{j2}) & \epsilon_{j1}(1 - \epsilon_{g2}) & \epsilon_{g1}(1 - \epsilon_{j2}) & \epsilon_{g1}(1 - \epsilon_{g2}) \\ \epsilon_{j1}\epsilon_{j2} & \epsilon_{j1}\epsilon_{g2} & \epsilon_{g1}\epsilon_{j2} & \epsilon_{g1}\epsilon_{g2} \end{pmatrix}. \quad (2)$$

where  $\epsilon_{g1}$  and  $\epsilon_{g2}$  are the fractions of the leading and sub-leading photons that have passed the event selection requirements pass the  $O_{NN} > 0.85$  cut, and  $\epsilon_{j1}$  and  $\epsilon_{j2}$  are the fractions of jets that have passed the event selection requirements pass the  $O_{NN} > 0.85$  cut.  $(N_{\gamma\gamma}, N_{\gamma j}, N_{j\gamma}, N_{jj})$  can be obtained by solving the linear equation. Table I shows the results after applying the method on the real data.

Total events	14670
$\gamma\gamma$	$4607 \pm 397$
$\gamma j + j\gamma$	$5025 \pm 557$
$jj$	$5038 \pm 496$

TABLE I: The number of  $\gamma\gamma$ ,  $\gamma j + j\gamma$ ,  $jj$  events in the data samples from the 4x4 matrix method. The quoted uncertainties include statistical uncertainties only.

## V. SYSTEMATIC UNCERTAINTIES

There are two dominant systematic uncertainties in this analysis: one is from electron track pointing inefficiency, the other is from the uncertainties of the estimation of  $\gamma + jet$  and  $jet + jet$  contributions. Additional uncertainties are the uncertainty on the total luminosity and the influence of the parton distribution functions (PDF) uncertainty on the acceptance depending on the Higgs mass, estimated from CTEQ6M [15] error functions. Table II lists all the systematic uncertainties of this analysis:

source	uncertainty
luminosity	6.1% [14]
PDF for $h \rightarrow \gamma\gamma$ acceptance	1.2% - 1.5%
ID efficiency	0.20% - 0.92%
photon "no-track" efficiency	0.31% - 1.56%
$Z/\gamma^*(ee)$ cross section	3.94%
electron track match inefficiency	10% - 15%
QCD $\gamma\gamma$ cross section	20%
$\gamma$ -jet and jet-jet estimation	26%

TABLE II: Uncertainties of this analysis are listed. The luminosity uncertainty is treated as correlated between signal and all backgrounds, also the ID efficiency uncertainty is treated as correlated between signal and  $Z/\gamma^*(ee)$  background and QCD  $\gamma\gamma$  background, and the uncertainty of photon "no-track" efficiency is treated as correlated between signal and QCD  $\gamma\gamma$  background.

## VI. FINAL EVENT DISTRIBUTIONS AND LIMITS

### A. Final event distributions

After the event selection, we show some kinematics distributions of the events in data together with those of the background estimation and signal (0.801 pb cross section and 100% branching ratio ( $h \rightarrow \gamma\gamma$ ) are used) in Fig. 2. The discrepancy between data and background estimation at small  $\Delta\phi(\gamma_1, \gamma_2)$  is believed to be a known problem in PYTHIA. It is shown in [12, 13] that PYTHIA can get the shape of the diphoton mass distribution right, but not  $\Delta\phi(\gamma_1, \gamma_2)$ . It significantly under-estimates the contribution at small  $\Delta\phi(\gamma_1, \gamma_2)$ .

### B. Limit setting

Since there is no evidence for new physics, we use the  $CL_s$  method [16, 17] to set 95% confidence level (C.L.) limits on the  $\sigma \times BR$  for different SM Higgs masses. The distribution of invariant mass of the two photon candidates in the interval of (50 GeV, 250 GeV) is used as the input to the limit setting code. The degrading effects of systematic uncertainties are reduced by introducing a maximum likelihood fit to the invariant mass distribution. Table III shows the number of events in data and the background estimation in the mass interval. The limits and selection efficiencies ( $\epsilon_{select}$ ) for different Higgs masses are shown in Table IV. Fig. 3 shows the obtained limits as a function of the Higgs mass.

data	13827
$Z/\gamma^* \rightarrow ee$	$740.9 \pm 102.3$
jet+jet	$4778.6 \pm 1264.6$
$\gamma$ +jet	$4677.2 \pm 1245.8$
QCD $\gamma\gamma$	$3400.5 \pm 711.0$
total background	$13597.2 \pm 2548.5$

TABLE III: Number of events in data and the background estimation in the mass interval of (50 GeV, 250 GeV). The jet+jet and  $\gamma$ +jet background contributions are estimated from the data, and thus have correlated statistical fluctuations with respect to the data. A few uncertainties are fully correlated among the various background contributions and the correlations are taken into account when computing the uncertainty of the total background. Thus the uncertainty of the sum of the background contributions are greater than the individual uncertainties added in quadrature.

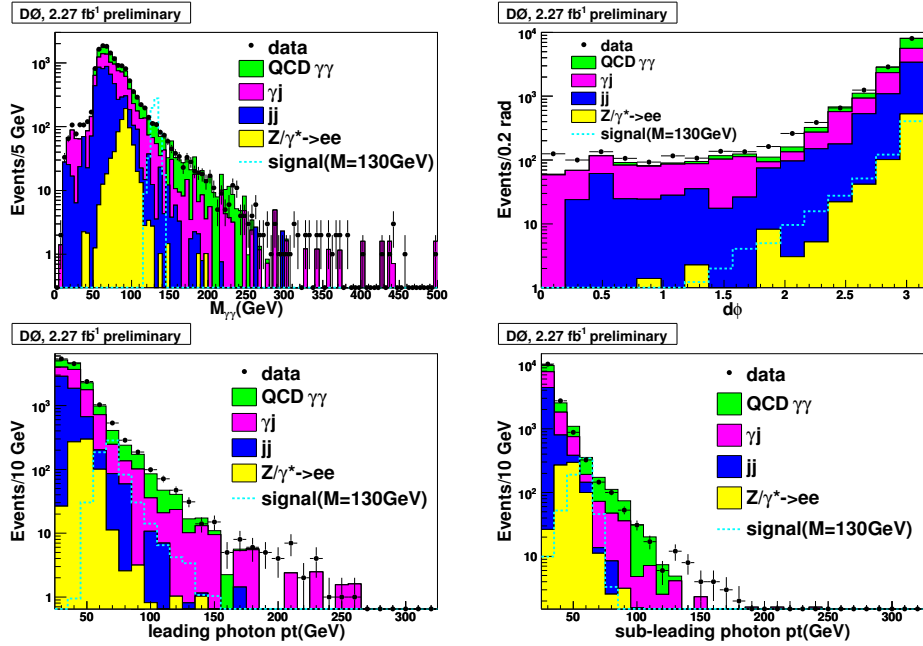


FIG. 2: Top-left is the invariant mass distribution and top-right is the  $\Delta\phi(\gamma_1, \gamma_2)$  distribution of two photon candidates, bottom-left is the  $p_T$  distribution of leading photon candidate, and bottom-right is the  $p_T$  distribution of the sub-leading photon candidate.

Higgs mass(GeV)	$\epsilon_{select}$	observed limits (fb)	expected limits (fb)
100	$0.1713 \pm 0.0035$	202.61	167.55
110	$0.1812 \pm 0.0034$	124.68	124.02
120	$0.1881 \pm 0.0035$	117.95	95.00
130	$0.1943 \pm 0.0033$	87.21	84.21
140	$0.1997 \pm 0.0035$	118.73	67.46
150	$0.2058 \pm 0.0035$	97.61	56.13

TABLE IV: The selection efficiencies with statistical uncertainties and 95% C.L. limits on  $\sigma \times BR$  (fb) for the different SM Higgs masses.

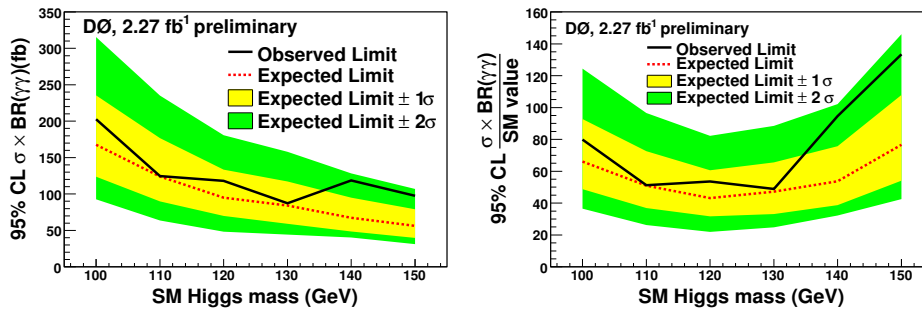


FIG. 3: Left plot shows the limits on the  $\sigma \times BR$  versus SM Higgs mass, right plot shows the limits as a ratio to the SM  $\sigma \times BR$  for different Higgs masses.

## VII. SUMMARY

This note describes a search for a light Higgs boson in the di-photon channel in 2.27  $fb^{-1}$   $D\emptyset$  Run II data. The data and SM background estimation are consistent, so we set the 95% C.L. limits on the  $\sigma \times BR$  for different SM Higgs masses.

## Acknowledgments

We thank the staffs at Fermilab and collaborating institutions, and acknowledge support from the DOE and NSF (USA); CEA and CNRS/IN2P3 (France); FASI, Rosatom and RFBR (Russia); CAPES, CNPq, FAPERJ, FAPESP and FUNDUNESP (Brazil); DAE and DST (India); Colciencias (Colombia); CONACyT (Mexico); KRF and KOSEF (Korea); CONICET and UBACyT (Argentina); FOM (The Netherlands); STFC (United Kingdom); MSMT and GACR (Czech Republic); CRC Program, CFI, NSERC and WestGrid Project (Canada); BMBF and DFG (Germany); SFI (Ireland); The Swedish Research Council (Sweden); CAS and CNSF (China); and the Alexander von Humboldt Foundation.

- 
- [1] S. Mrenna and J. Wells, arXiv:hep-ph/0001226
  - [2] A. Heister et al. (ALEPH Collaboration), Phys. Lett. B **544**, 16 (2002).
  - [3] P. Abreu et al. (DELPHI Collaboration), Phys. Lett. B **507**, 89 (2001); Eur. Phys. J. C **35**, 313, (2004).
  - [4] G. Abbiendi et al. (OPAL Collaboration), Phys. Lett. B **544**, 44 (2002).
  - [5] P. Achard et al. (L3 Collaboration), Phys. Lett. B **534**, 28 (2002); Phys. Lett. B **568**, 191 (2003).
  - [6]  $D\emptyset$  Collaboration, "Search for Light Higgs Boson in  $\gamma\gamma+X$  Final State with the  $D\emptyset$  Detector at  $\sqrt{s} = 1.96$  TeV",  $D\emptyset$  Note **5426-CONF** (2007).
  - [7] V. M. Abazov et al., Nucl. Instrum. Meth. A **565**, 463 (2006).
  - [8] C. Peterson, T. Rognvaldsson and L. Lonnblad, "JETNET 3.0 A versatile Artificial Neural Network Package", Lund University Preprint LU-TP 93-29. Version 3.5 is used here.
  - [9] T.Sjöstrand et al., hep-ph/0108264,LU-TP-01-21,Lund2001
  - [10] R. Hamberg, W. L. van Neerven and T. Matsuura, Nucl. Phys. B **359**, 343 (1991) [Erratum-ibid. B **644**, 403 (2002)].
  - [11] T. Binoth, J. Ph.Guillet, E. Pilon, and M. Werlen, Eur. Phys. J. C. **16**, 311 (2000).
  - [12] Y. Liu, Ph.D. thesis, Fermilab [FERMILAB-THESIS-2004-37] (2004).
  - [13] D. Acosta et al. (CDF collaboration), Phys. Rev. Lett. **95**, 022003 (2005).
  - [14] T. Andeen et al., FERMILAB-TM-2365 (2007).
  - [15] J. Pumplin et al., JHEP **0207**, 012 (2002).
  - [16] W. Fisher, FERMILAB-TM-2386-E (2006).
  - [17] T. Junk, Nucl. Instrum. Meth. A **434**, 435 (1999); A. Read, CERN 2000-005 (30 May 2000).